Physics-Based Phase Noise Analysis of CMOS RF Oscillators

Sung-Min Hong, Chan Hyeong Park†, Myoung Jin Lee, Hong Shick Min, and Young-June Park

School of EECS and Nano-System Institute (NSI-NCRC), Seoul National University, San 56-1, Sillim-dong, Gwanak-gu, Seoul 151-744, Korea.
Telephone: +82-2-880-7285, Fax: +82-2-882-4658, E-mail: hi2ska2@isis.snu.ac.kr
†Dept. of Electronics and Communications Eng., Kwangwoon University, Seoul, Korea

Abstract

A physics-based phase noise analysis and simulation of CMOS RF oscillators is reported. The device-circuit mixed-mode simulation is employed to obtain the periodic steady-state of the oscillator. The influence of noise sources inside the devices on the oscillator's phase noise is calculated using the perturbation projection vector for the first time. Detailed simulation results are shown for a CMOS LC oscillator.

1. Introduction

An accurate phase noise analysis and simulation of CMOS RF oscillators is very important to design low-noise CMOS RF communication systems. Although many efforts have been made to address this subject, a rigorous understanding of phase noise phenomenon due to the white noise sources in oscillators has been developed quite recently [1].

In the circuit simulation, some commercial RF simulators (such as Cadence SpectreRF) implement the phase noise analysis algorithms. However, accuracy of the compact device models (CM) can still be a problem for an accurate circuit-level simulation mainly because the CM does not reflect the detailed physics inside the device especially for the device from newly developed technology. A device-circuit mixed-mode simulator has the potential to provide simulation results exploiting more accurate numerical device models.

In this paper, we report a physics-based phase noise analysis of CMOS RF oscillators using the device-circuit mixed-mode simulator.

2. Device-Circuit Mixed-Mode Simulation

The device-circuit mixed-mode simulator, CLESICO [2], has been extended to calculate the periodic steady-state of the oscillator. In this simulator, the semiconductor equations (Poisson's equation and continuity equations for electrons and holes) for each device in the circuit are discretized as in the conventional device simulators. A lumped circuit element is characterized by its terminal voltages and currents. The whole device-circuit system is represented in a fully-coupled manner.

An artificial voltage source is imposed to start up the oscillator. After an initial transient simulation during an appropriate time interval is carried out, the 'matrix-free' shooting-Newton method [3] is exploited to find the periodic steady-state of the oscillator. Also the period of oscillation is added to the set of unknown variables.

3. PPV Calculation for Phase Noise Analysis

The perturbation projection vector (PPV) [1,4] method is adopted to analyze the phase noise of the oscillator. The PPV, which is a T-periodic vector, represents the effects of noise sources on the time derivative of the oscillator phase deviation. According to this method, the phase noise or jitter can be characterized by the per cycle jitter, c. Calculation of the PPV is a primary nontrivial step to obtain the phase noise spectrum. In this work, we exploited the time-domain computation algorithms in [4] for calculation of the PPV.

4. Simulation Results and Discussion

Simulation has been carried out for a CMOS LC oscillator. The circuit schematic considered in the simulation is shown in Fig. 1. Two NMOSFETs and one PMOSFET are treated as 2D semiconductor devices. The quality factors of two inductors are set to be about 3. We will concentrate on three node voltages (node #3, #4 and #7) and the physical quantities of the left NMOSFET.

Fig. 2 shows the voltage waveforms in an initial transient simulation during 10 nsec. Using the transient solution as an initial guess, we perform the periodic steady-state simulation. The oscillation period T, is found to be 2.081 nsec. Fig. 3 shows the voltage waveforms of the calculated periodic steady-state. Fig. 4 shows the magnitudes of Fourier coefficients of the oscillator output voltage, which is the voltage difference between node #3 and #4. Electron concentration at the oxide-silicon interface of the left NMOS is plotted as a function of time in Fig. 5. In this figure, the x-axis (–90 nm ~ 90 nm) denotes the lateral position. The drain region is located from 45 nm to 90 nm in the x-axis. The y-axis (0 nsec ~ 2.081 nsec) denotes one clock cycle.

We perform the PPV calculation using the periodic steady-state. Fig. 6 shows the PPV for Kirchhoff's current law at three circuit nodes. Figs. 7, 8, 9 and 10 show the PPV for electron continuity equation in the left NMOS at t = 0.2 T, 0.4 T, 0.6 T and 0.8 T, respectively. The y-axis (0 nm ~ 100 nm) denotes the vertical position while the x-axis denotes the lateral position. The oxide-silicon interface is located at 0 nm in the y-axis. As shown in these figures, the PPV inside a MOSFET at a certain time looks similar to the drain current Green's function [2,5]. Fig. 11 shows the PPV for electron continuity equation at the oxide-silicon interface in the left NMOS as a function of time. For a comparison, the PPV for Poisson's equation is plotted in Fig. 12.

In this example, we consider diffusion noise sources for electrons and holes in three MOSFETs and thermal noise sources for inductors' parasitic resistors. In the case of diffusion noise sources, we should calculate the inner product of the gradient of the PPV and the diffusion noise source vector as in the Green's function technique [5]. Including colored noise sources (such as g-r noise source and flicker noise source) in the physics-based noise simulation is a topic of future research.

Fig. 13 shows the contributions of noise sources in two NMOSFETs to the per cycle jitter, c, as a function of time. The contributions of noise sources in other devices (such as inductors and PMOSFET) are found to be negligible in this example. Fig. 14 shows a time average of spatial contribution of electron diffusion noise sources in the left NMOSFET to the per cycle jitter, c. The contribution has its peak value at the near-source region in the channel. Integrating the spatial contribution over the device volume, we can calculate the per cycle jitter, c, which is essential in phase noise characterization. The value of c is calculated to be 1.5098 fsec.

We calculate the power spectral density of the output voltage. Fig. 15 shows the computed output voltage power spectral density around lowest four harmonics. Fig. 16 shows the computed output voltage power spectral density around the first harmonic. The power spectral density clearly shows a Lorentzian shape.

5. Conclusion

In this work, we reported a physics-based phase noise analysis of the CMOS RF oscillators. The phase noise characteristic of a LC oscillator has been simulated. It was found that the PPV inside a MOSFET at a certain time looks similar to the drain current Green's function. The output power spectral density originated from the diffusion noise sources and thermal noise sources showed a Lorentzian shape. Authors expect that this framework can be a useful tool for an accurate phase noise analysis in the CMOS RF oscillators.

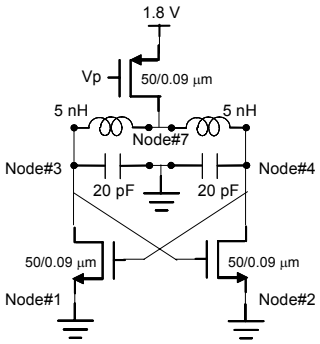

Fig. 1: Schematic of CMOS LC oscillator simulated.

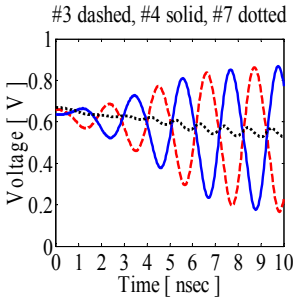

Fig. 2: Voltage waveforms in an initial transient simulation.

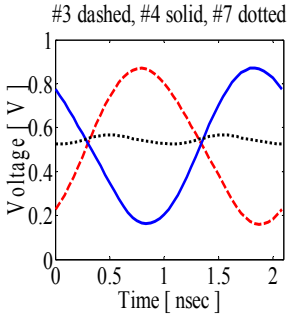

Fig. 3: Voltage waveforms of the periodic steady-state.

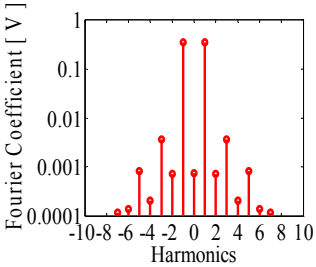

Fig. 4: Magnitudes of Fourier coefficients of the oscillator output voltage.

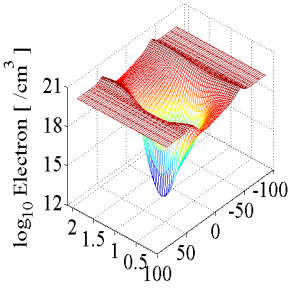

Fig. 5: Electron concentration at the oxide-silicon interface of the left NMOS as a function of time. See the text for an explanation of the x- and y-axes.

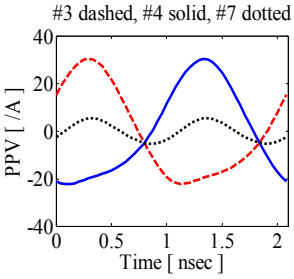

Fig. 6: PPV for Kirchhoff's current law.

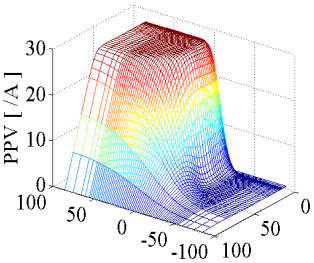

Fig. 7: PPV for the electron continuity equation in the left NMOSFET at t = 0.2 T. See the text for an explanation of x- and y-axes.

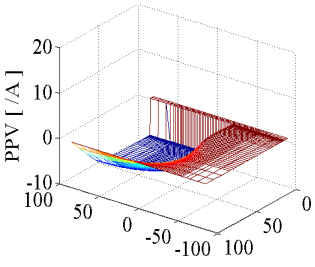

Fig. 8: Same quantity as in Fig. 7 at t = 0.4 T.

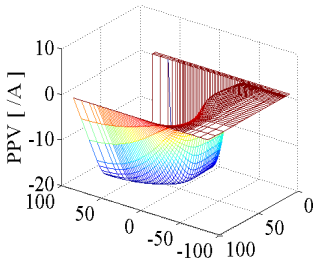

Fig. 9: Same quantity as in Fig. 7 at t = 0.6 T.

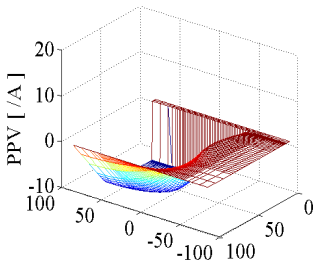

Fig. 10: Same quantity as in Fig. 7 at t = 0.8 T.

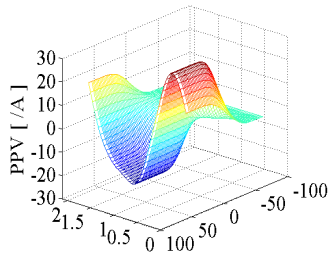

Fig. 11: PPV for the electron continuity equation at the oxide-silicon interface in the left NMOSFET as a function of time. The x- and y-axes are the same as those in Fig. 5.

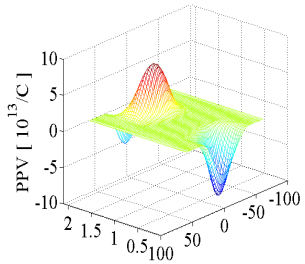

Fig. 12: PPV for Poisson's equation at the oxide-silicon interface in the left NMOSFET as a function of time. The x- and y-axes are the same as those in Fig. 5.

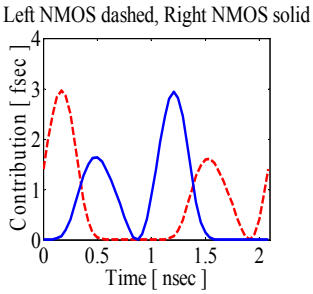

Fig. 13: Contributions of noise sources in two NMOSFETs to the per cycle jitter, c, as a function of time.

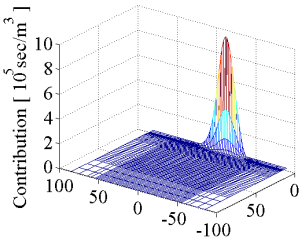

Fig. 14: Time average of spatial contribution of the electron diffusion noise sources in the left NMOSFET to the per cycle jitter, c. The x- and y-axes are the same as those in Fig. 7.

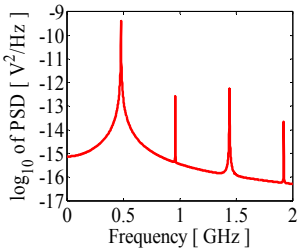

Fig. 15: Computed output voltage power spectral density around lowest four harmonics.

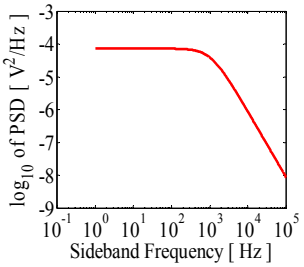

Fig. 16: Computed output voltage power spectral density around the first harmonic.

References

[1] A. Demir, et. al, IEEE T. CAS – I, vol. 47, pp. 655 - 674, 2000.
[2] S.-M. Hong, et. al, SISPAD, pp. 119 - 122, 2005.
[3] R. Telichevesky, et. al, DAC, pp. 480 – 484, 1995.
[4] A. Demir, et. al, IEEE T. CAD, vol. 22, pp. 188 - 197, 2003.
[5] F. Bonani, et. al, IEEE T. ED, vol. 45, pp. 261 - 269, 1998.